Quantum Chemical Analysis of the Energetics of the anti- and gauche-Conformers of Ethanol

Article *in* Structural Chemistry · February 2009

DOI: 10.1007/s11224-008-9395-7 · Source: OAI

2 authors:

Steve Scheiner
Utah State University
431 PUBLICATIONS **20,098** CITATIONS
SEE PROFILE

Paul Grant Seybold
Wright State University
124 PUBLICATIONS **5,276** CITATIONS
SEE PROFILE

Struct Chem (2009) 20:43–48
DOI 10.1007/s11224-008-9395-7

ORIGINAL RESEARCH

Quantum chemical analysis of the energetics of the *anti* and *gauche* conformers of ethanol

Steve Scheiner · Paul G. Seybold

Received: 29 October 2008 / Accepted: 27 November 2008 / Published online: 11 December 2008

Abstract Ethanol displays two stable conformers, the classic *anti* (or *trans*) form and a *gauche* conformation in which the hydroxyl hydrogen points toward one of the methyl hydrogens. Surprisingly, the two forms have nearly equal energies, and in the vapor phase the *gauche* form predominates because of its twofold degeneracy. An analysis of the energetics of these conformers based on natural bond orbital analysis helps to explain the apparently anomalous near degeneracy of these conformers.

Keywords Rotamers · Lone pairs · NBO · Charge transfer

Introduction

Ethanol was among the first organic chemicals to be synthesized and remains today a classic organic chemical, an important industrial product, a key biofuel, and a molecule of astronomical interest [1]. It has long been recognized that the ethanol molecule itself can exist in two stable rotameric forms, *anti* (or *trans*) and *gauche*, although in textbooks [2] and other venues [3] the molecule is almost always depicted in its paradigmatic *anti* form. Historically, because of instrumental and other experimental limitations, most early studies of ethanol focused almost exclusively on the *anti* conformer, although by the 1970s experimental studies confirmed the presence of the stable *gauche* form [4–6].

An early study by Barnes and Hallam [7] estimated the ratio of *anti* to *gauche* conformers at room temperature in the vapor phase to be roughly 2:1. However, a microwave study by Kakar and Quade [8], a far-IR study by Durig and Larsen [9], and a 1996 microwave study by Pearson et al. [10] have all indicated that the energy of the *gauche* form lies only about 40 cm^{-1} above that of the *anti* conformer, so that one might expect a preponderance of the gauche form at room temperature because of its two-fold degeneracy. An IR/VCD study has indeed reported a 42:58 *anti*/*gauche* ratio for the two conformers [11].

Theoretical studies of the two conformers, although differing in specific details, have generally shown the two conformers to have closely comparable energies. Indeed, even changes in basis set or application of electron correlation can cause a reversal in the order [12], and vibrational effects can also play a major role [11]. For example, using a 4-21G basis set Van Alsenoy et al. [13] found the *gauche* form to be more stable by 0.15 kcal/mol. A study by Görbitz [12] using second-order Møller–Plesset perturbation theory (MP2) with a 6-311G** basis set also showed the *gauche* conformer to be slightly lower in energy. However, an MP4/6-31+G** calculation by Shaw et al. [11] found the *anti* form to be more stable by 0.52 kJ/mol. A more recent density functional theory B3LYP/6-311++G** study by Coussan et al. [14] places the *anti* conformer 0.42 kJ/mol lower in energy than the *gauche* conformer. Senent et al. [15] used Dunning's correlation consistent triple zeta basis set with Møller–Plesset perturbation theory up to MP4 and obtained the *anti* form falling 19 cm^{-1} below the *gauche* form. Weibel et al. [16] have carried out a number of higher-level ab initio calculations including coupled cluster calculations, and found that both

S. Scheiner (✉)
Department of Chemistry and Biochemistry,
Utah State University, Logan, Utah 84322-0300, USA
e-mail: scheiner@cc.usu.edu

P. G. Seybold
Departments of Chemistry and Biochemistry,
Wright State University, Dayton, Ohio 45435, USA

MP4 and CCSD(T) single-point calculations place the *gauche* form about 0.13 kcal/mol below the *anti* form. These workers also noted that the narrower potential well for the *gauche* torsion results in a zero-point energy larger by about 113–125 cm^{-1} for this form, which can reverse the order. Some representative calculated energies for the two conformers are given in Table 1.

It is thus clear from both experimental and theoretical perspectives that the *anti* and *gauche* conformers of ethanol have very nearly equal energies. What is curious about this finding is that whereas in the *anti* form the hydroxyl hydrogen points symmetrically away from the methyl hydrogen atoms, thereby avoiding contact with these atoms, inspection of the *gauche* form shows that its –OH hydrogen is oriented directly toward one of the methyl hydrogens, an orientation that might be expected to have a notably unfavorable effect on the energy.

There have been attempts to rationalize this surprisingly small energy difference over the years. As one example, an early proposal [17] explained OH frequency shifts [18] by suggesting that an oxygen lone pair can delocalize into the CH σ^* antibonding orbital when the two are anti to one another, thereby weakening the CH bond, and shifting its stretching frequency to the red. Despite the experimental and theoretical scrutiny that these forms have received over several decades, so far as we are aware no satisfactory explanation for the surprising near degeneracy of these two conformers and the geometry of the *gauche* form has been presented. Here, we examine the energetic influences prevailing in these conformers and suggest an explanation for their nearly equal energies and for the apparently counterintuitive geometry of the *gauche* form.

Calculations

The calculations reported here were performed using Spartan06 (Wavefunction, Inc., 18401 Von Karman Ave., Suite 370, Irvine, CA 92612) and the Gaussian03 suite [19] of programs. Several different basis sets were applied, all of which were internal to the computer codes. Geometries were fully optimized, with no restrictions. Wave functions were analyzed using the NBO formalism of Reed et al. [20] [21, 22].

Results

It is sometimes thought that the *gauche* structure ought to be higher in energy than the *anti* rotamer by virtue of a closer contact between the hydroxyl H atom H_0 and the methyl H labeled H_{b1} in Fig. 1. However, this interatomic distance is about 2.5 Å in the optimized *gauche* structure, as indicated in Table 1. This relatively long interhydrogen distance, 0.1 Å greater than the sum of the van der Waals radii, would argue for only very minimal steric repulsion. Moreover, the closest –OH···H contacts are actually those with the C_α hydrogens, H_{a1} and H_{a2}, for both the *anti*

Table 1 Difference in energy (*gauche–anti*) and geometric details calculated for ethanol by different methods

Level	ΔE (kJ/mol)	$r(H_o-H_{b1})$[a] gauche (Å)	$\varphi(CCOH_o)$[a] gauche (degs)	Refs.
HF 6-31G*	−0.45	2.548	63.8	b
HF 6-311+G**	−1.18	2.549	62.6	b
B3LYP/6-31G*	1.33	2.540	61.6	b
B3LYP/6-311G**	1.05	2.534	60.7	b
B3LYP/6-311++G**	−0.17	2.549	60.0	b
B3LYP/cc-pVTZ	0.13	2.543	60.4	b
MP2/6-31+G*	−0.72	2.534	60.9	b
MP2/6-311++G**	0.06	2.472	57.0	b
MP2/cc-pVTZ	−0.28	2.493	60.0	b
MP2/6-311++G(3df,3pd)	0.97	2.506	60.8	b
MP2/cc-pVQZ	1.03	2.496	60.0	b
MP2/aug-cc-pVQZ	1.04	2.500	60.0	b
MP4/6-31+G**	−0.52			c
CCSD(T)/6-311++G**	0.49			d

[a] Atomic labeling from Fig. 1

[b] This work

[c] Ref. [11]

[d] Ref. [17]

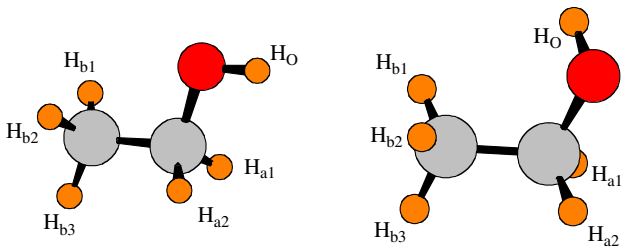

(a) anti **(b)** gauche

Fig. 1 *Anti* and *gauche* conformers of ethanol, showing atomic labeling used below

(2.34 Å, two contacts) and the *gauche* (2.35 Å, one contact) conformers.

One might seek hints as to the near degeneracy of the two conformers in the details of the covalent bond lengths. The differences between *gauche* and *anti* bond lengths are reported in Table 2 using several different basis sets, all at the MP2 level. The positive entries in the first row indicate that the hydroxyl O–H_o bond is nearly 1 mÅ longer in the *gauche* conformer when compared to the *anti* value. Two of the largest differences occur for the C–C bond, which is about 6 mÅ longer in the *gauche* form, and the C–O, bond, which is 2–3 mÅ shorter. Within the subset of C–H bonds, the C–H_{a2} bond shows the greatest change, about 5 mÅ shorter in *gauche*, followed by the 2.5 mÅ lengthening of C–H_{b1}. There are certain aspects of these trends which are intriguing. The change in the C–H_{b1} bond length is certainly understandable in light of the much closer approach of H_o to this atom in the *gauche* arrangement. On the other hand, it is not obvious from the outset why the C–H_{a2} bond should be so sensitive to C–OH rotation, as the H_o atom is not situated very close to H_{a2} in either structure.

In order to obtain some insights into the underlying reasons for the changes in bond lengths, NBO analysis was carried out on the wave functions associated with the *anti* and *gauche* geometries. Of particular interest was the possibility of charge transfer into the antibonding orbitals of each of these bonds. The energetic consequence of such charge transfer is measured via $E(2)$, the second-order perturbation theory component, which is defined as

$$E_{ij}(2) = q_i\left(F_{ij}^2/\varepsilon_j - \varepsilon_i\right), \quad (1)$$

where q refers to the donor orbital occupancy, F_{ij} to the off-diagonal NBO Fock matrix element, and ε_i to the orbital eigenvalue. For each bond, the values of all charge transfers into the relevant antibonding orbital were added together to arrive at a total charge transfer energy for that particular bond.

Taking the C–H_{a2} bond as an example, in the *anti*-geometry there are three orbitals which transfer charge into its σ^* orbital. There is an energy contribution of 2.64 kcal/mol arising from the C–H_{b1} bonding orbital. Another 9.34 kcal/mol comes from the two O lone pair orbitals; of the latter sum, 8.40 kcal/mol, or 90%, is attributable to the O lone pair that is essentially a *p*-orbital, perpendicular to the C–O–H_o plane, and that nearly eclipses the C–H_{a2} bond. Altogether, there is a total of 11.94 kcal/mol resulting from charge transfer into the C–H_{a2} antibond in the *anti* configuration. Turning next to the *gauche* structure, there are again three orbitals that transfer charge into the C–H_{a2} antibond. The C–H_{b1} bonding orbital contributes 2.54 kcal/mol, not very different from its 2.64 in the *anti* structure. The O–H bond makes another contribution, in the amount of 2.46 kcal/mol. There is only one O lone pair (a sort of sp^2 hybrid that eclipses the C–H_{a2} bond) that contributes, in the amount of 3.62 kcal/mol. The total of these three contributions is 8.62 kcal/mol, smaller by 3.32 kcal/mol than in the case of the *anti* structure. It is this value that is reported as the last entry in Table 2, which lists the difference in $E(2)$ between the *gauche* and *anti* structures for each bond.

Indeed, the change in the total charge transfer energy, on going from *anti* to *gauche*, does appear to correlate quite well with the change in the length of each bond. This correlation is evident in Fig. 2 where the values of $\Delta E(2)$ in the last column of Table 2 for all the different bonds are

Table 2 Differences in bond lengths and sums of $E(2)$, between *gauche* and *anti* conformers (G–A), calculated at MP2 level

	Δr^a (mÅ)				$\Delta E(2)^b$
	6-31+G**	6-311++G(3df,3pd)	cc-pVQZ	aug-cc-pVQZ	kcal/mol
O–H_o	0.7	0.8	0.6	0.7	1.14
C–O	−1.3	−3.0	−1.8	−3.0	−1.64
C–C	6.3	6.1	5.6	5.9	4.43
C–H_{b1}	2.5	2.6	2.5	2.7	0.27
C–H_{b2}	0.1	0.2	0.0	0.3	0.07
C–H_{b3}	0.5	1.0	1.0	1.0	0.16
C–H_{a1}	0.5	0.6	0.1	0.5	0.34
C–H_{a2}	−5.7	−5.0	−5.4	−5.0	−3.32

[a] *Gauche–anti*

[b] Computed with aug-cc-pVQZ basis set

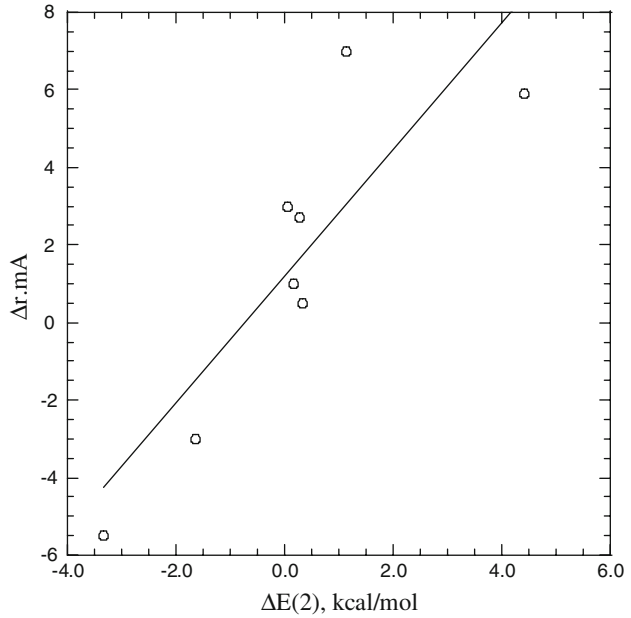

Fig. 2 Linear correlation between gauche-anti bond length differences and NBO charge transfer $\Delta E(2)$

compared with the bond length elongation or contraction in the preceding column of the table. In all cases, an increase of charge transfer into a given bond's antibonding orbital correlates with an elongation, and a presumed weakening, of the bond while a lowering of transfer into the antibond shortens and strengthens this bond. The linear relationship is fair, with a correlation coefficient $r = 0.863$. The slope of the best-fit straight line is such that each 1 kcal/mol increase in charge transfer energy corresponds to an elongation of the pertinent bond by 1.15 mÅ.

What is perhaps apparent from the above discussion of the C–H_{a2} antibonding orbital is that the contributing orbitals all lie roughly parallel to the bond in question. That is, in the context of the *anti* structure, the C–H_{b1} bond is anti (180°) to the C–H_{a2} bond, and the O lone pair that is the major contributor (*p*-orbital) is roughly parallel to C–H_{a2}. Likewise in the case of the *gauche* geometry, the bonds that are anti to C–H_{a2} are C–H_{b1} and O–H_o. Since one of the two O lone pairs is orthogonal to C–H_{a2} in the *gauche* structure, charge transfer into its antibonding orbital is very severely diminished (by 61%). Considering the O–H_o bond as another example, it is not surprising that its contributors are the C–C bond in the *anti* conformer and C–H_{a2} in the *gauche* conformer. This pattern in which the major components of charge transfer arise from orbitals that are coplanar to one another is in fact the dominating factor in the trends observed in both charge transfer and bond length.

Finally, we turn our attention to the fundamental distinctions between the *anti* and *gauche* structures, with respect to the idea that charge transfer, as described above, can help stabilize or destabilize the system. Bearing in mind that the lone pairs are better suited to release charge than are the covalent bonds, due to the constrained nature of the latter, we focus our attention on the orientation of the two O lone pairs, whose orientations are illustrated in Fig. 3 for the two configurations. The NBO localized description of the wave function provides for two different orbitals, which would fit into the general notion of sp^2 hybridization of the O atom. Thus one lone pair, LP1, corresponds to the third sp^2 orbital, lying in the C–O–H_o plane. LP2 represents the third *p*-orbital of O, which is perpendicular to the latter plane. The numbers displayed in Fig. 3 represent the charge transfer energy $E(2)$ (in kcal/mol) from each lone pair to the indicated C–H or C–C antibond. The charge transfers associated with LP1 are fairly modest. The largest value, 3.62 kcal/mol, occurs for the C–H_{a2} antibond in the gauche configuration. The size of this contribution may be attributed to the fact that this lone pair very nearly eclipses the C–H_{a2} bond, i.e. the dihedral angle is 0°. The *p*-orbital, LP2, seems much more capable of transferring charge, with quantities in excess of 8 kcal/mol. Most importantly, these large degrees of transfer occur for those C–H and C–C bonds which are most closely aligned with the *p*-orbital. The charge transfers are equal to 8.40 kcal/mol for the C–H_{a1} and C–H_{a2} antibonds in the *anti* configuration, while there is no such transfer into C–C which is orthogonal to LP2. A similar pattern is evident for the *gauche* structure, where the C–H_{a1} and C–C antibonds are now the recipients of charge transfer, while the orthogonal C–H_{a2} antibond receives none. In summary then, the charge transfer from the O lone pairs is maximized by a roughly coplanar alignment with the recipient antibond.

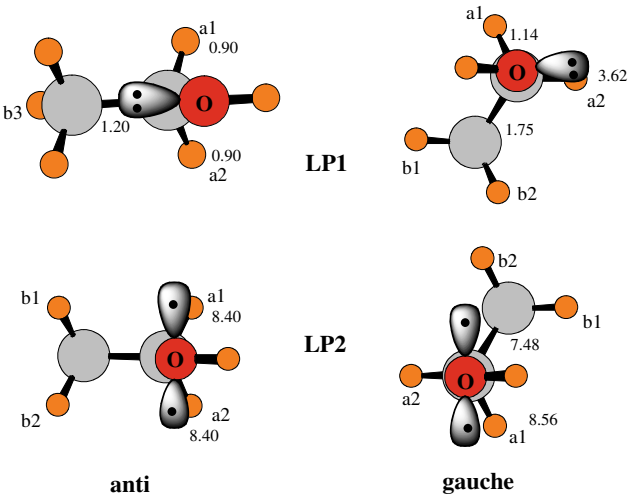

Fig. 3 Disposition of two localized lone pairs in the *anti* and *gauche* conformers. LP1 refers to sp^2-type lone pair, and LP2 to *p*-orbital. The amount of charge transfer energy $E(2)$ from the indicated lone pair to the labeled CH and CC antibonds are included, in kcal/mol

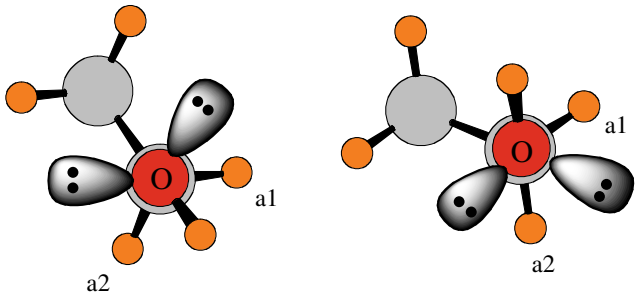

Fig. 4 Disposition of two equivalent sp^3 "rabbit ear" O lone pairs in the *anti* and *gauche* conformers

Table 3 Total charge transfer energy ($E(2)$, kcal/mol) into indicated antibonds, arising from O lone pairs

Antibond	*Anti*	*Gauche*
CH_{a1}	9.30	9.70
CH_{a2}	9.30	3.62
C–C	1.20	9.23

There has been some discussion in the literature as to whether the two hydroxyl O lone pairs are better described as the aforementioned sp^2 hybrid and *p*-orbital, or as a pair of equivalent "rabbit ears" that would follow from an sp^3-hybridization of the oxygen atom [23, 24]. In fact, the two descriptions are equivalent as one is related to the other by a unitary transformation of the total wave function. It follows that a rabbit-ear description ought to obey the same patterns of charge transfer as does the sp^2 hybrid and *p*-orbital description. Figure 4 illustrates the sp^3-disposition of lone pairs from which it may be observed that there is a lone pair anti to the C–H_{a1} bond, for both the *anti* and *gauche* structures. Since the anti (or syn) arrangement of the charge-donating lone pair and the accepting antibond corresponds to a planar alignment, with a zero dihedral angle, it is hence not surprising to note from the first row of Table 3 that the charge transfer into the C–H_{a1} antibond from the O lone pairs is about the same for both conformers. In the case of C–H_{a2}, however, this C–H bond is anti to a lone pair in the *anti* conformer, but there is no such anti lone pair in the *gauche* structure. There is consequently a strong diminution in the lone pair charge transfer, by a factor of nearly three, on going from *anti* to *gauche*, as documented in the second row of Table 3. The trend in the C–C bond is just the opposite, in that the lone pair transfer is much larger in the *gauche* structure, which is easily explained by the presence of an O lone pair anti to C–C in *gauche*, but not in the *anti* conformer. The dominating influence of the two O lone pairs is reinforced by inspection of Table 2 which reveals that it is the aforementioned C–C and C–H_{a2} bonds that undergo by far the largest changes in both bond length and $\Delta E(2)$.

In summary, then, one can explain the near degeneracy of the *anti* and *gauche* conformers by a compensatory effect. The *anti* structure is stabilized by charge transfer from the O lone pairs into the C–H_{a1} and C–H_{a2} bonds that are each trans to one of the lone pairs. Internal rotation into the *gauche* conformer retains the C–H_{a1} interaction, and simply replaces the C–H_{a2} charge transfer with a like process that involves the C–C bond. We note in passing that in related compounds additional influences may substantially shift the conformer equilibrium. In 2,2,2-trifluoroethanol, for example, where –OH···F attractions are present, calculations at the B3LYP/6–311++G** level show the *gauche* form to be more stable by 9 kJ/mol, and in 2,2,2-trichloroethanol the calculations show the *gauche* form to be more stable by 12 kJ/mol.

References

1. Pearson JC, Sastry KVLN, Herbst E, De Luca FC (1997) Astrophys J 175:246–261
2. McMurry J (2000) Organic Chemistry, 5th edn. Brooks/Cole, Pacific Grove, CA, p 655 See, for example
3. American Chemical Society "Molecule of the Week", June 25, 2007. See http://portal.acs.org/portal/acs/corg/content
4. Michielsen J (1969) J Mol Spectrosc 29:489–491. doi:10.1016/0022-2852(69)90126-X
5. Sasada Y, Takano M, Satoh T (1971) J Mol Spectrosc 38:33–42. doi:10.1016/0022-2852(71)90091-9
6. Durig JR, Bucy WE, Wurrey CJ, Carreira LA (1975) J Phys Chem 79:988–993. doi:10.1021/j100577a009
7. Barnes AJ, Hallam HE (1970) Trans Faraday Soc 66:1932–1940. doi:10.1039/tf9706601932
8. Kakar RK, Quade CR (1980) J Chem Phys 72:4300–4307. doi:10.1063/1.439723
9. Durig JR, Larsen RA (1989) J Mol Struct 238:195–222. doi:10.1016/0022-2860(90)85015-B
10. Pearson JC, Sastry KVLN, Herbst E, De Luca FC (1996) J Mol Spectrosc 480:420–431
11. Shaw RA, Wieser H, Dutler R, Rauk A (1990) J Am Chem Soc 112:5401–5410. doi:10.1021/ja00170a002
12. Görbitz CH (1992) J Mol Struct THEOCHEM 262:209–218. doi:10.1016/0166-1280(92)85109-X
13. Van Alsenoy C, Scarsdale N, Williams JO, Schäfer L (1982) J Mol Struct 86:365–376
14. Coussan S, Bouteiller Y, Perchard JP, Zheng WO (1998) J Phys Chem 102:5789–5793
15. Senent ML, Smeyers YG, Dominguez-Gómez R, Villa M (2000) J Chem Phys 112:5809–5819. doi:10.1063/1.481155
16. Weibel JD, Jackels CF, Swofford RL (2002) J Chem Phys 117:4245–4254. doi:10.1063/1.1496472
17. Krueger PJ, Jan HWJ (1970) J Mol Struct 5:375–387. doi:10.1016/0022-2860(70)80043-6
18. Bakke JM, Bjerkeseth LH (1997) J Mol Struct 407:27–38. doi:10.1016/S0022-2860(96)09726-8
19. Frisch MJ, Trucks GW, Schlegel HB, Scuseria GE, Robb MA, Cheeseman JR, Zakrzewski VG, Montgomery JA Jr., Stratmann RE, Burant JC, Dapprich S, Millam JM, Daniels AD, Kudin KN,

Strain MC, Farkas O, Tomasi J, Barone V, Cossi M, Cammi R, Mennucci B, Pomelli C, Adamo C, Clifford S, Ochterski J, Petersson GA, Ayala PY, Cui Q, Morokuma K, Malick DK, Rabuck AD, Raghavachari K, Foresman JB, Cioslowski J, Ortiz JV, Baboul AG, Stefanov BB, Liu G, Liashenko A, Piskorz P, Komaromi I, Gomperts R, Martin RL, Fox DJ, Keith T, Al-Laham MA, Peng CY, Nanayakkara A, Gonzalez C, Challacombe M, Gill PMW, Johnson B, Chen W, Wong MW, Andres JL, Gonzalez C, Head-Gordon M, Replogle ES, Pople JA (2003) Gaussian03. Gaussian, Inc., Pittsburgh PA

20. Reed AE, Curtiss LA, Weinhold F (1985) J Chem Phys 83:735–746. doi:10.1063/1.449486
21. Reed AE, Weinhold F, Curtiss LA, Pochatko DJ (1986) J Chem Phys 84:5687–5705. doi:10.1063/1.449928
22. Reed AE, Curtiss LA, Weinhold F (1988) Chem Rev 88:899–926. doi:10.1021/cr00088a005
23. Liang M (1987) J Chem Educ 64:124–128
24. Martin RB (1988) J Chem Educ 65:668–670